nature catalysis

SUPPLEMENTARY INFORMATION

https://doi.org/10.1038/s41929-019-0264-0

In the format provided by the authors and unedited.

# Perfluorocarbon nanoemulsion promotes the delivery of reducing equivalents for electricity-driven microbial $CO_2$ reduction

**Roselyn M. Rodrigues, Xun Guan, Jesus A. Iñiguez, Daniel A. Estabrook, John O. Chapman, Shuyuan Huang, Ellen M. Sletten and Chong Liu***

Department of Chemistry and Biochemistry, University of California, Los Angeles, Los Angeles, CA, USA. *e-mail: chongliu@chem.ucla.edu

Supplementary Information

# Perfluorocarbon Nanoemulsion Promotes the Delivery of Reducing Equivalents for Electricity-driven Microbial $CO_2$ Reduction

Roselyn M. Rodrigues[1], Xun Guan[1], Jesus A. Iñiguez[1], Daniel A. Estabrook[1], John O. Chapman[1], Shuyuan Huang[1], Ellen M. Sletten[1], Chong Liu[1,*]

[1] Department of Chemistry and Biochemistry, University of California, Los Angeles, Los Angeles, CA 90095, USA

*To whom correspondence may be addressed. Email: chongliu@chem.ucla.edu

Address: 607 Charles E Young Dr. E, Los Angeles, CA 90095, USA

*Index* *Page*

## Supplementary Methods

### Characterizations with Flow Cytometry

Experiments of flow cytometry were performed on a Biorad S3e cell sorter with a sample volume of 1.00 mL when two excitation lasers on the instrument (488 and 561 nm, 100mW for both) were turned on. The percentage of the trigger signal, threshold, that would be counted as a single and individual event was 1%. The 488 nm laser was used to collect the signals of forward scattering (FSC) and side scattering (SSC). The photomultiplier tube (PMT) settings for FSC and SSC were 350 and 250 V, respectively. The 561 nm excitation laser was applied to the FL2 detector, which detects 585/25 nm wavelengths. The FL2 detector had a PMT setting of 900 V. 20,000 events were collected for each sample during the measurement. The FL2 detector was used to collect the emission of rhodamine fluorophore at 571 nm under the excitation of 561 nm laser. As an internal standard, polystyrene microspheres from the Invitrogen™ LIVE/DEAD™ *Bac*Light™ bacterial viability and counting kit for flow cytometry were used under a dilution ratio of 1:100 to achieve in a final concentration of 1 x $10^6$ beads per mL. All data was analyzed using a FlowJo software (version 10). The blank samples containing only the polystyrene microspheres (Fig. 3B) were used to distinguish the range of SSC-area for the population of microspheres. Subsequently, samples with *S. ovata* (Fig. 3A) were analyzed to determine the range of SSC-area for the microbial population. These gate settings were used to evaluate the populations for other samples (Fig. 3C and 3D).

Living cultures of *S. ovata* after a three-day incubation were prepared as outlined above for the experiments. Minimal medium, which described in the section "Medium Recipes of Microbial Cultures", was prepared anaerobically with the addition of reducing agent and was subsequently mixed with polystyrene micropsheres (1:100 dilution) along with various combinations of *S. ovata* culture and/or fluorescently tagged PFC nanoemulsion whose preparation was listed above. Our reported data is from results with a dilution ratio of 1:50 for microbial culture. We attempted dilution ratios of PFC nanoemulsion between 1:10 and 1:1000, and the reported data is from results with a dilution ratio of 1:10 in order to obtain a large enough population of signals from PFC nanoemulsion.

**List of samples tested**

| Figures | Nanoemulsion | Cultures of *S. ovata* | Microspheres |
|---|---|---|---|
| Fig. 3B | - | - | + |
| Fig. 3C | + | - | + |
| Fig. 3A | - | + | + |
| Fig. 3D | + | + | + |

The unidentified SSC low population marked as * in Fig. 3B is from the medium solution and mostly likely due to the residual particles that were not completely removed during the filtration process. Although these signals overlap with the ones of bacteria shown in Fig. 3A, these unidentified signals have minimal interference with other measurements. As stated in above, the concentration of microspheres as an internal standard are the same among all the samples (1:100

dilution) and a total of 20,000 events were collected for each sample during the measurements. In Fig. 3B, the microspheres accounts for 45.3% of all the events, and the rest is attributed to the residual particles. In contrast, in Fig. 3A, only 3.7% of the 20,000 events is from the microspheres and 92.4% of events is correlated with the addition of bacterial culture. This suggests that the unidentified events from the medium solution only contributes about 4.6% of the counts in Fig. 3A. Therefore, a predominant majority of the SSC low population in Fig. 3A indeed represented the added bacteria, and our conclusion of a non-specific binding with the microbes remains valid.

**Analysis of Experiments with Rotating Disk Electrode**

The Koutechý-Levich plot is governed by the equation below,[1]

$$\frac{1}{j} = \frac{1}{j_k} + \frac{1}{0.62nFD^{2/3}\nu^{-1/6}C_o}\omega^{-1/2} \quad (1)$$

In this equation, $j$ is the current density, $j_k$ the kinetic current density, $n$ is the number of electrons involved in the electrochemical reaction, $F$ the Faraday's constant, $D$ the diffusion coefficient, ν is the kinematic viscosity, $C_o$ is the concentration of the species being reacted at the electrode, and ω is the spin rate. Specifically, in our case, $n = 2$ for electrochemical $H_2$ oxidation. The y-intercepts in the Koutechý-Levich plots lead us to conclude that the values of $j_k$ were 12.9 mA/cm$^2$ and 3.7 mA/cm$^2$ for solutions without and with PFC nanoemulsions, respectively. In order to obtain the effective concentration of $H_2$ from the Koutechý-Levich equation, the kinematic viscosity ν and diffusion coefficient of $H_2$, $D$, needed to be determined.

*Measurement of kinematic viscosities.* The kinematic viscosity was experimentally determined with a Fisherbrand™ Glass Kinematic Viscometer following the procedures in ASTM D 446. Three measurements were performed for each sample and the average results were used in our analysis. For water, ν = 1.04 x $10^{-6}$ m$^2$/s. For 0.5% PFC nanoemulsion, ν = 1.06 x $10^{-6}$ m$^2$/s.

*Determination of Diffusion Coefficients.* The diffusion coefficients were determined using diffusion-ordered spectroscopy (DOSY) $^1$H NMR Bruker AV300 at the Molecule Instrumentation Center in UCLA. with 0.5% PFC nanoemulsion was prepared using $D_2O$ as the solvent so that there would be no interference from $H_2O$ signal (4.7 ppm). Attempts to conduct the experiments with solvent suppression in $D_2O/H_2O$ mixture (20/80) were unsuccessful. The DOSY spectra were obtained at 30 ºC with a diffusion time (Δ) of 50 ms, a diffusion gradient length (δ) of 1.5 ms, a recycle delay between scans of 2 s, and the maximum gradient was 50 gauss·cm$^{-1}$. The spectra are reported in log of diffusion coefficient (m$^2$·s$^{-1}$) versus chemical shift (ppm). The signals analyzed were at 4.5 ppm and the diffusion coefficients with and without nanoemulsion were determined to be $2.0\times10^{-9}$ m$^2$/s and $4.5\times10^{-9}$ m$^2$/s, respectively (Supplementary Fig. 11). Due to the differences of viscosities between $H_2O$ and $D_2O$, the diffusion coefficients of gases measured in $D_2O$ can be about 15% lower than the values in $H_2O$ at 30 ºC.[2] Such a systematic uncertainty will not change the conclusions when we compared the data both derived from the RDE experiments, as the measurement uncertainty from $D_2O$ should equally impact liquid media with and without PFC nanoemulsion, given the small volume percentage of added PFC (2.5%). Yet as the diffusion coefficient $D$ scales on the order of −2/3 in the Koutechý-Levich equation, this systematic uncertainty will pose a relative uncertainty of about 11% when we compare the bulk value of $H_2$ concentration in PFC nanoemulsion with the one calculated from the RDE experiments.

*Calculations of effective $H_2$ concentrations.* Using the values determined above and the slopes in the Koutechý-Levich plots from the RDE experiments, the effective concentrations of $H_2$ were calculated to be 0.99 mM for the nanoemulsion and 0.63 mM for the control under an environment of $H_2/CO_2$ (80/20) mixture at 1 bar. These values correspond to 0.78 and 1.24 mM for nanoemulsion and control under a $H_2$ pressure of 1 bar.

**Medium Recipes of Microbial Cultures**

*DSMZ 311 MEDIUM*

| | |
|---|---|
| $NH_4Cl$ | 0.50 g |
| $MgSO_4$ • 7 H2O | 0.50 g |
| $CaCl_2$ • 2 $H_2O$ | 0.25 g |
| NaCl | 2.25 g |
| $FeSO_4$ • 7 $H_2O$ | 0.002g |
| Trace element solution SL-10 (see below) | 1.00 ml |
| Selenite-tungstate solution (see below) | 1.00 ml |
| Yeast extract | 2.00 g |
| Casitone | 2.00 g |
| Betaine • $H_2O$ | 6.70 g |
| Na-resazurin solution (0.1% w/v) | 0.50 ml |
| $K_2HPO_4$ | 0.35 g |
| $KH_2PO_4$ | 0.23 g |
| $NaHCO_3$ | 4.00 g |
| Vitamin solution (see below) | 10.00 ml |
| Distilled water | 1000.00 ml |

All ingredients (except phosphates, bicarbonate, vitamins, cysteine and sulfide) were dissolved first. And the medium was sparged with $N_2/CO_2$ (80/20) gas mixture while boiling to make the solution anoxic. Once cool, and while still sparging with the same gas, phosphates, vitamins (sterilized by filtration) and carbonate were added. The medium was dispensed under the same gas into anaerobic culture tubes and then autoclaved. The pH of the complete medium was adjusted to pH 7.0, if necessary.

*TRACE ELEMENT SOLUTION (SL-10)*

| | |
|---|---|
| Nitrilotriacetic acid | 1.50 g |
| $MgSO_4$ • 7 $H_2O$ | 3.00 g |
| $MnSO_4$ • $H_2O$ | 0.50 g |

| | |
|---|---|
| NaCl | 1.00 g |
| $FeSO_4 \cdot 7\ H_2O$ | 0.10 g |
| $CoSO_4 \cdot 7\ H_2O$ | 0.18 g |
| $CaCl_2 \cdot 2\ H_2O$ | 0.10 g |
| $ZnSO_4 \cdot 7\ H_2O$ | 0.18 g |
| $CuSO_4 \cdot 5\ H_2O$ | 0.01 g |
| $KAl(SO_4)_2 \cdot 12\ H_2O$ | 0.02 g |
| $H_3BO_3$ | 0.01 g |
| $Na_2MoO_4 \cdot 2\ H_2O$ | 0.01 g |
| $NiCl_2 \cdot 6\ H_2O$ | 0.03 g |
| $Na_2SeO_3 \cdot 5\ H_2O$ | 0.30 mg |
| Na2WO4 • 2 $H_2O$ | 0.40 mg |
| Distilled water | 1000.00 ml |

The nitrilotriacetic acid was first dissolved and the pH adjusted to 6.5 with KOH, then the minerals were added. The final pH was adjusted to pH 7.0 with KOH.

*VITAMIN SOLUTION*

| | |
|---|---|
| Biotin | 2.00 mg |
| Folic acid | 2.00 mg |
| Pyridoxine-HCl | 10.00 mg |
| Thiamine-HCl • 2 H2O | 5.00 mg |
| Riboflavin | 5.00 mg |
| Nicotinic acid | 5.00 mg |
| D-Ca-pantothenate | 5.00 mg |
| Vitamin B12 | 0.10 mg |
| p-Aminobenzoic acid | 5.00 mg |
| Lipoic acid | 5.00 mg |
| Distilled water | 1000.00 ml |

*SELENITE-TUNGSTATE SOLUTION*

| | |
|---|---|
| NaOH | 0.5 g |
| $Na_2SeO_3 \cdot 5\ H_2O$ | 3.0 mg |
| $Na_2WO_4 \cdot 2\ H_2O$ | 4.0 mg |

| | |
|---|---|
| Distilled water | 1000.0 ml |

*REDUCING AGENT SOLUTION*

All the water used in this procedure was boiled and gassed under $N_2$ prior to the experiments. 12.5 g cysteine-HCl was dissolved in 500 mL water in a 2-L Erlenmeyer flask. The pH of the solution was adjusted to 9.5 with NaOH. 12.5 g of washed crystals of $Na_2S{\cdot}9H_2O$ was weighted in a plastic tray and then transferred into the flask containing cysteine-HCl. The volume of the solution was brought up to 1000 mL. The whole solution was brought to boil and cool again under gassing with $N_2$. 20 mL of the prepared solution was dispensed into one 25-mL vial which was pre-flushed with $N_2$. The vials were sealed and then autoclaved for 15 min at 121 $^oC$.

*BASELINE MEDIUM*

| | |
|---|---|
| $K_2HPO_4$ | 0.348 g |
| $KH_2PO_4$ | 0.227 g |
| $Na_2HPO_4 \bullet 7H_2O$ | 2.145 g |
| $NaH_2PO_4 \bullet H_2O$ | 0.938 g |
| $NH_4Cl$ | 0.500 g |
| $MgSO_4 \bullet 7H_2O$ | 0.500 g |
| $CaCl_2 \bullet 2H_2O$ | 0.250 g |
| NaCl | 0.918 g |
| $FeSO_4 \bullet 7H_2O$ | 0.002 g |
| $NaHSeO_3$ | 10-7 mol/L |
| $NaHCO_3$ | 4.000 g |
| SL-10 solution | 1 mL |
| Vitamin solution | 10 mL |
| Yeast extract | 2.000 g |

Compared to the DSMZ-recommended growth medium, the concentration of phosphate buffer was increased by 5 times from 3.7 mM to 18.5 mM without changing the overall $K^+$ and $Na^+$ concentration. All ingredients (except phosphates, bicarbonate, vitamins, cysteine and sulfide) were dissolved first. And the medium was sparged with $N_2/CO_2$ (80/20) gas mixture while boiling to make the solution anoxic. Once cool, and while still sparging with the same gas, phosphates, vitamins (sterilized by filtration) and carbonate were added. The medium was dispensed under the same gas into anaerobic culture tubes and then autoclaved. The pH of the complete medium was adjusted to pH 7.0, if necessary. High-salinity medium was prepared based on the recipe above, while the concentration of the phosphate buffer was increased three-fold from 18.5 mM to 55.5 mM. Minimal medium, which was used in the experiments of flow cytometry, was prepared following the same procedure as the baseline media, however it only included $NH_4Cl$, NaCl, $K_2HPO_4$, $KH_2PO_4$, and $NaHCO_3$.

## Supplementary Discussion

### Estimation of the energy expenses with the addition of PFC nanoemulsion

We estimated the energy demand for the production of PFC and compared with the energy gains in the process of $CO_2$ reduction. We conclude that the energy expenses of PFC are not significant as compared to the net gain of $CO_2$ reduction, as long as the PFC nanoemulsion can be recycled for multiple runs.

We estimated the energy expenses in the production of PFC nanoemulsions by dividing the energy cost into two components. The first component is energy cost of producing PFC molecules ($\Delta E_1$) and the second one is the energy demand of producing PFC nanoemulsions from bulk chemicals ($\Delta E_2$).

The Gibbs formation energies of the PFCs used in this manuscript were estimated based on the Joback method:[3] *n*-PFH, $\Delta_f G^\circ = -2710.7$ kJ/mol; PFD, $\Delta_f G^\circ = -3516.7$ kJ/mol. As the industrial process of PFC synthesis is not well reported, we calculated the energy expenses of these compounds from the most available commodity chemicals, graphite for the carbon element and hydrofluoric acid for the fluorine element. Based on such assumptions, the reaction free energies and hence the $\Delta E_1$ are calculated as:

PFH: $6\ C(s) + 14\ HF\ (g) \rightarrow C_6F_{14}\ (l) + 7\ H_2\ (g) \quad \Delta E_{1,1} = 1145.6\ kJ/mol$ (2)

PFD: $10\ C(s) + 18\ HF\ (g) \rightarrow C_{10}F_{18}\ (l) + 9\ H_2\ (g) \quad \Delta E_{1,2} = 1440.5\ kJ/mol$ (3)

In our experiments, the solution contains 2.5 % PFC with a 1:1 ratio between perfluorohexane and perfluorodecaline. Therefore, the thermodynamic energy cost of producing PFCs are $\Delta E_1$ = +8.2 kJ for the 0.1 L solution with 2.5 % PFC used in the experiments.

We also calculated the energy demand of producing PFC nanoemulsions from bulk chemicals. Experimentally, 3 watts of energy were supplied for 5 min to prepare emulsions that were later diluted into a 1 L solution. Subsequently $\Delta E_2$ equals about 90 J for 0.1 L solution with 2.5 % PFC.

The process of electrochemical $CO_2$ reduction into acetate has the following thermodynamic balance:

$2\ CO_2\ (g) + 2\ H_2O\ (l) \rightarrow CH_3COOH\ (aq) + 2\ O_2(g) \quad \Delta_r G = +839.0\ kJ/mol$ (4)

Experimentally about 0.64 g (0.011 mmol) of acetic acid was produced from a 0.1-L reactor in 4 days. This corresponds to a net energy gain of 9.2 kJ, which is slightly higher than the 8.2 kJ required for the production of PFC and the preparation of nanoemulsions. Such a comparison implies that the payback time of energy expenses for the addition of PFC nanoemsulison is about 3.5 days. Given that the PFC compounds phase separate with aqueous media easily and can be re-used for the preparation of nanoemulsion with almost negligible energy cost (~ 90 J for every 4 days), the energy expenses of PFC is not significant as compared to the net gain of $CO_2$ fixation.

### Contribution of direct electron transfer (DET) from microbes

While *S. ovata* is reported to exhibit direct electron transfer (DET) on the electrode surface without the generation of $H_2$ gas, such a process is not considered to be significant in the experiments.[4,5] DET requires a direct close contact between electrodes and microbes.[6] Our experiments proceeded

with bacteria well dispersed in the bulk solution. Moreover, there was no visible biofilm formation on the electrodes, possibly due to the generation of $H_2$ gas bubbles and the stirring in the reactor.

We do not consider that the capability of conducting DET in *S. ovata* contributes to our observed kinetic enhancement. One working hypothesis of DET suggests some "metallic" redox-transporting proteins on cell membranes and/or pili.[6] The interfacial chemistry between PFC nanoemulsions and microorganisms is not well understood. But it is reasonable to assume that the interface between microbes and nanoemulsion contains a significant amount of surfactant, Pluronic F68. Our experiments of rotating disk electrode (RDE) indicate that the redox-inactive Pluronic F68 indeed inhibits the kinetics of $H_2$ oxidation (Supplementary Fig. 10). Therefore, a process analogous to the DET on electrodes is unlikely to take place at the interface of nanoemulsions. Subsequently, the capabilities of conducting DET in *S. ovata* is unlikely to contribute to the reported discovery.

**Supplementary Table 1.** List of experiments reported in this work [a]

| Entry | PFC nanoemulsion (v/v, %) | E° [b] (mV vs. SHE) | *j* (mA/cm$^2$) | Titer (g·L$^{-1}$) | $r_{CO2}$ (g·L$^{-1}$·d$^{-1}$) | $r_{CO2}$' (g·m$^{-2}$·d$^{-1}$) | *F. E.* (%) |
|---|---|---|---|---|---|---|---|
| *1* | 0 | −871 | −0.50 ± 0.09 | 1.59 ± 0.49 | 0.39 ± 0.10 | 32.2 ± 8.0 | 94 ± 15 |
| *2* | 2.5 | −911 | −0.58 ± 0.07 | 1.59 ± 0.26 | 0.38 ± 0.12 | 31.9 ± 10.0 | 90 ± 16 |
| *3* | 0 | −961 | −1.14 ± 0.14 | 2.63 ± 0.30 | 0.65 ± 0.25 | 54.0 ± 20.5 | 71 ± 8 |
| *4* | 2.5 | −971 | −1.05 ± 0.16 | 3.17 ± 0.47 | 0.78 ± 0.11 | 64.7 ± 8.9 | 92 ± 8 |
| *5* | 0 [c] | −1001 | −2.01 ± 0.16 | 2.23 ± 0.29 | 0.54 ± 0.13 | 44.8 ± 11.2 | 33 ± 2 |
| *6* | 2.5 [c] | −1021 | −1.99 ± 0.05 | 6.39 ± 1.14 | 1.58 ± 0.44 | 132.0 ± 36.7 | 99 ± 19 |
| | 0 [d] | −981 | −1.45 ± 0.0001 | 0.96 ± 0.40 | 0.23 ± 0.15 | 19.1± 12.6 | 20 ± 8 |
| | 2.5 [d] | −1001 | −1.67 ± 0.0001 | 0.59 ± 0.17 | 0.13 ± 0.07 | 10.6 ± 5.9 | 9 ± 4 |

[a] General conditions: *S. ovata* (DSM 2662) is used as the biocatalyst; Co-P alloy loaded on SS mesh (both sides, 2 cm × 3 cm). The reported data here are the results during four-day experiments. Baseline medium was used unless mentioned specifically. $n \geq 3$. The errors denote standard error of the mean (SEM). [b] The reported voltages was the averaged values from all replicates. [c] High-salinity medium which contains 55.5 mM phosphate buffer. [d] Slow microbial growth was observed.

**Supplementary Table 2.** List of previous reports for pure cultures of *Sporomusa ovata* in electricity-driven microbial $CO_2$ fixation.

| Strain of *S. ovata* | Cathode | $E^{\circ}$ (mV *vs.* SHE) | $j$ (mA/cm$^2$) | $t$ (d) | Titer (g·L$^{-1}$) | $r_{CO2}$ (g·L$^{-1}$·d$^{-1}$) | $r_{CO2}$' (g·m$^{-2}$·d$^{-1}$) | *F. E.* (%) | Ref |
|---|---|---|---|---|---|---|---|---|---|
| *DSM 2662* [a] | Graphite stick | −400 | −0.0695 [d]<br>−0.0207 [e] | 6 | 0.0625 | 0.01 [EV]<br>0.045 [STY] | 4.64[d]<br>1.38[e] | 85 | *7* |
| *DSM 2662* [b] | Chitosan-coated CC | −400 | −0.0475 [d] | 9 | 0.59 | 0.065 ± 0.16 | 2.75 ± 0.67[d] | 82 ± 12 | *8* |
| *DSM 2662* [b] | Ni-coated nanowire | −400 | −0.218 [d]<br>−0. 65 [e] | 8 | 0.54 | 0.068 | 11.35[d]<br>3.38[e] | 82 ± 14 | *9* |
| *DSM 2662* [c] | Si-$TiO_2$ nanowire | −595 to −571 | −0.35 [d]<br>−0.012 [e] | 5 | 1.2 | 0.24 | N. D. [f] | 86 ± 9 | *4* |
| *DSM 2662* [b] | Reduced Graphene Oxide paper | −690 | −0.258 ± 0.054 [d] | 12 | N. D. [f] | N. D. [f] | 10.11 ± 1.34 [d] | 91 ± 9 | *10* |
| *DSM 2662* [b] | Carbon paper | −690 | −0.037 ± 0.010 [d] | 12 | N. D. [f] | N. D. [f] | 1.20 ± 0.30 [d] | 84 ± 4 | *10* |
| *DSM 2662* [b] | Carbon felt | −690 | −0.040 ± 0.010 [d] | 12 | N. D. [f] | 0.019 ± 0.006 | 1.02 ± 0.33 [d] | 77 ± 2 | *11* |
| *DSM 2662* [b] | 3D-Graphene on Carbon felt | −690 | −0.245 ± 0.016 [d] | 12 | N. D. [f] | 0.125 ± 0.004 | 6.95 ± 0.22 [d] | 87 ± 3 | *11* |
| *DSM 2662* [b] | Carbon Cloth | −690 | −0.03 ± 0.01 [d] | 14 | 0.2 | N. D. [f] | 1.64 ± 0.27 [d] | 87 ± 7 | *12* |
| *DSM 2662* [b] | PEDOT: PSS on Carbon cloth | −690 | −0.32 ± 0.08 [d] | 14 | 1.6 | N. D. [f] | 15.15 ± 1.06 [d] | 79 ± 6 | *12* |
| *DSM 2662* [b] | Graphite stick | −690 | −0.045 ± 0.015 [d] | 14 | 0.51 | 0.029 ± 0.006 [d] | 2.06 ± 0.42 [d] | 92 ± 5 | *13* |
| *DSM 2663* [b] | Graphite stick | −690 | −0.078 ± 0.019 [d] | 14 | 0.99 | 0.053 ± 0.016 [d] | 3.67 ± 1.09 [d] | 61 ± 12 | *13* |
| *DSM 3300* [b] | Graphite stick | −690 | −0.019 ± 0.0005 [d] | 14 | 0.20 | 0.011 ± 0.005 [d] | 0.77 ± 0.34 [d] | 85 ± 4 | *13* |
| N. A. [b,g] | Graphite disk | −660 | −0.017 ± 0.004 [d] | 28 | 0.54 | 0.020 ± 0.003 [d] | 1.68 ± 0.24 [d] | 105 ± 5 | *14* |

The errors denote SEM. [a] Estimates based on continuous feed linear production and flow rates reported (EV is rate calculated per exit volume, STY is the space-time yield). [b] Estimates based on batch operation (volume in cathode chamber). [c] Light as energy source. [d] Based on projected surface area. [e] Based on total surface area. [f] N. D.: not determined. [g] N. A.: The specific strain information was not available in the report.

**Supplementary Table 3.** List of previous reports for other acetogen strains in electricity-driven microbial $CO_2$ fixation.

| Microorganism/ strain | Cathode | $E^{\circ}$ (mV *vs.* SHE) | $j$ (mA/cm$^2$) | $t$ (days) | Titer (g·L$^{-1}$) | $r_{CO2}$ (g·L$^{-1}$·d$^{-1}$) | $r_{CO2}$' (g·m$^{-2}$·d$^{-1}$) | *F.E.* (%) | Ref |
|---|---|---|---|---|---|---|---|---|---|
| *Sporomusa malonica DSM 5090* [a] | Graphite stick | −690 | −0.070 ± 0.017 [d] | 14 | 0.63 | 0.039 ± 0.004 [d] | 2.73 ± 0.29 [d] | 91 ± 14 | *13* |
| *Sporomusa acidovorans DSM 3132* [a] | Graphite stick | −690 | −0.057 ± 0.021 [d] | 14 | 0.72 | 0.038 ± 0.012 [d] | 2.65 ± 0.85 [d] | 70 ± 1 | *13* |
| *Sporomusa aerivorans DSM 13326* [a] | Graphite stick | −690 | −0.0026 ± 0.0002 [d] | 14 | N. D. [c] | N. D. [c] | N. D. [c] | N. D. [c] | *13* |
| *Sporomusa sphaeroides DSM 2875* [b] | Graphite stick | −400 | −0.057 [d] −0.017 [e] | 8 | 0.0028 | 0.00035 [EV] 0.0027 [STY] | 0.208 [d] 0.062 [e] | 39 | *7* |
| *Sporomusa silvacetica DSM 10669* [b] | Graphite stick | −400 | −0.02 [d] −0.006 [e] | 10 | 0.002 | 0.0002 [EV] 0.0025 [STY] | 0.15 [d] 0.045 [e] | 84 | *7* |
| *Clostridium aceticum DSM 1496* [b] | Graphite stick | −400 | −0.08 [d] −0.024 [e] | 13 | 0.0027 | 0.0002 [EV] 0.0042 [STY] | 0.02 [d] 0.006 [e] | 27 | *7* |
| *Clostridium ljungdahlii DSM 13528* [b] | Graphite stick | −400 | −0.104 [d] −0.031 [e] | 7 | 0.0065 | 0.0009 [EV] 0.0054 [STY] | 0.47 [d] 0.14 [e] | 72.2 ± 0.2 | *7* |
| *Clostridium ljungdahlii DSM 13528* [a] | Graphite felt + stainless steel | −695 | −1.0 [d] | 11 | 0.56 | 0.056 to 0.144 | 7.51 to 19.2 | 39-89 | *15* |
| *Moorella thermoacetica DSM 21394* [b] | Graphite stick | −400 | −0.03 [d] −0.009 [e] | 9 | 0.0047 | 0.0006 [EV] 0.0045 [STY] | 0.35 [d] 0.104 [e] | 85 ± 7 | *7* |
| *Acetobacterium woodii DSM 1030* [b] | Graphite stick | −400 | N. D. [c] | -- | N. D. [c] | N. D. [c] | N. D. [c] | N. D. [c] | *7* |
| *Acetobacterium woodii DSM 1030* [a] | Stainless steel felt | −690 | −1.5 [d] | 1 | 0.127 | 0.046 | 12.8 [d] | 81 | *16* |

The errors denote SEM. [a] Estimates based on batch operation (volume in cathode chamber ). [b] Estimates based on continuous feed linear production and flow rates reported (EV is rate calculated per exit volume, STY is the space-time yield). [c] N. D.: not determined or not reported. [d] Based on projected surface area. [e] Based on total surface area.

**Supplementary Table 4.** List of previous reports of the production of acetic acid combining electrolyzes with gas fermentation

| Microorganism/ strain | *t* (days) | Titer ($g \cdot L^{-1}$) | $r_{CO2}$ ($g \cdot L^{-1} \cdot d^{-1}$) | $r_{CO2}'$ ($g \cdot m^{-2} \cdot d^{-1}$) | *F. E.* (%) | Ref |
|---|---|---|---|---|---|---|
| *Clostridium autoethanogenum DSM 10061* [a,b] | 2 | 2.33 | 1.17 | N. D. [f] | 100 [g] | *17* |
| *Moorella thermoacetica DSM 6867* [a,b,c] | 7 | 30 | 26.4 | N. D. [f] | 3.7 | *18* |
| *Acetobacterium woodii DSM 1030* [b,d] | 3.2 | 21.7 | 18.24 | N. D. [f] | 10 | *19* |
| *Acetobacterium woodii DSM 1030* [b,d,e] | 3.2 | 17.6 | 147.84 | N. D. [f] | 56 | *19* |

[a] Estimates based on batch operation [b] Equipped with a pH auxostat system. [c] Bubble column reactor setup. [d] Continuous stirred-tank reactors (CSTR). [e] Hollow fiber membrane in the system. [f] N. D.: not determined or not reported. [g] reported as "almost 100%" without the exact values provided.

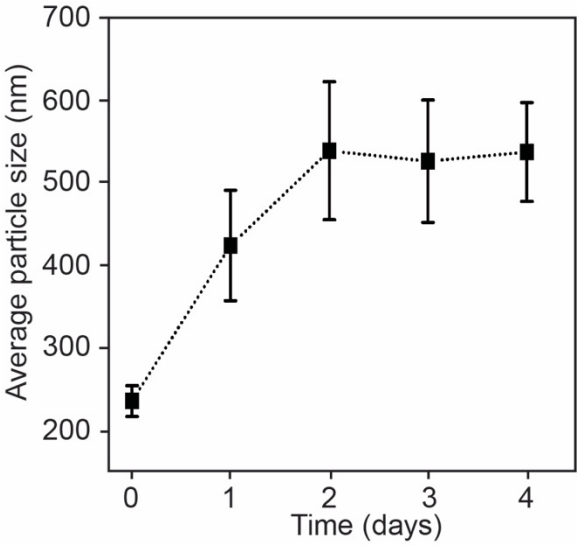


**Supplementary Fig. 1.** The change of average size of 2.5% PFC nanoemulsion over 4 days at 34°C in baseline medium. Detailed experimental conditions is listed in section "Dynamic Light Scattering". n ⩾ 3, the errors denote SEM.

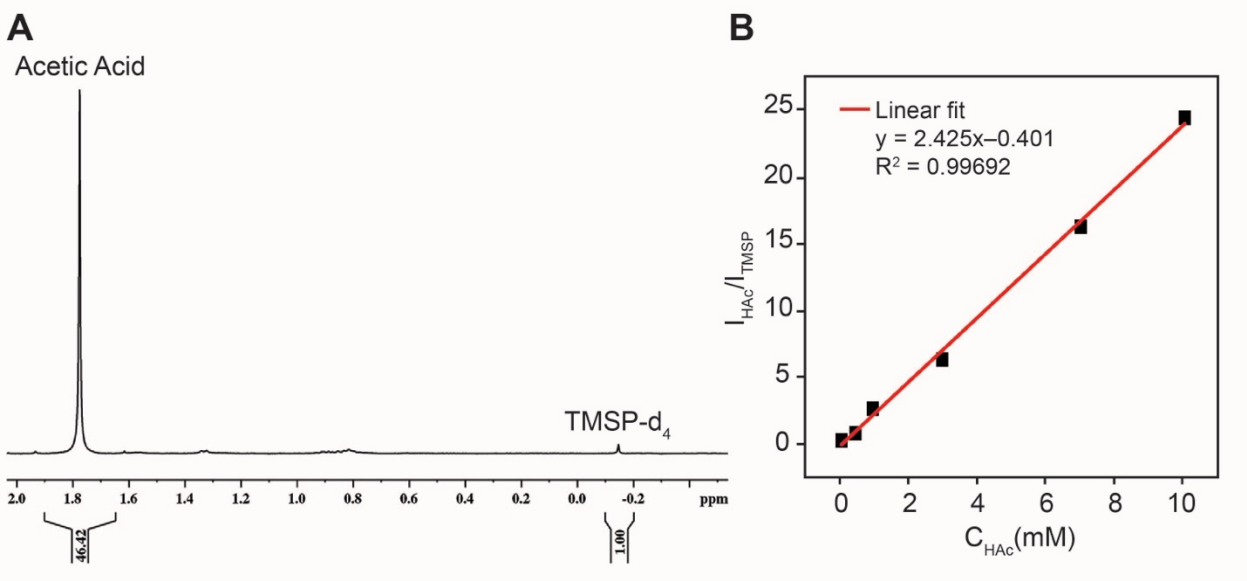


**Supplementary Fig. 2. a**, Representative $^{1}H$ NMR spectrum of a sample with the addition of internal standard, 2,2,3,3-D4 sodium-3-trimethylsilylpropionate (TMSP-$d_4$), in $D_2O$. **b**, Calibration curve that plots the ratio of integration area between acetate (1.77 ppm) and TMSP-$d_4$ (−0.15 ppm) *vs.* the concentrations of acetate in standard solutions.

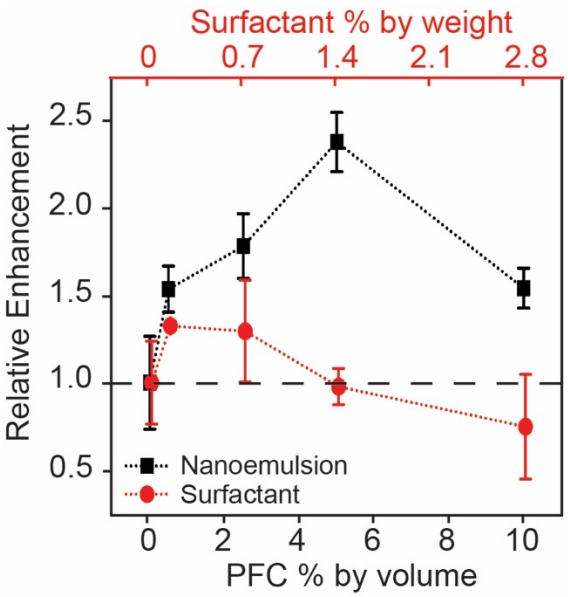


**Supplementary Fig. 3.** Viability test of *S. ovata* in PFC nanoemulsions. The relative enhancements of the accumulation of acetic acid by microbial $CO_2$ fixation are plotted against the volumetric percentage of PFC in the nanoemulsion (black). As the PFC nanoemulsion also contains surfactants that might interfere with experiments, results of the corresponding control experiments with only surfactant added (red) are also displayed. $n = 4$, the errors denote SEM.

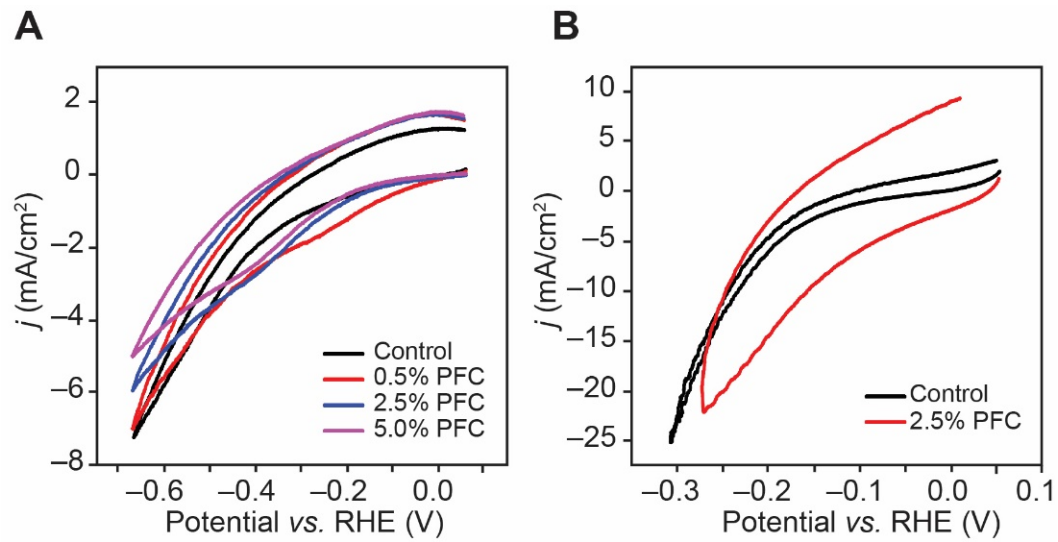


**Supplementary Fig. 4.** Cyclic voltammograms of Co-P alloy catalyst loaded on SS mesh substrate for varying percentages of PFC nanoemulsion in the baseline media (**a**) and 1 mol/L potassium phosphate buffer (**b**) at pH 7. The scan rate is at 10 $mV \cdot s^{-1}$.

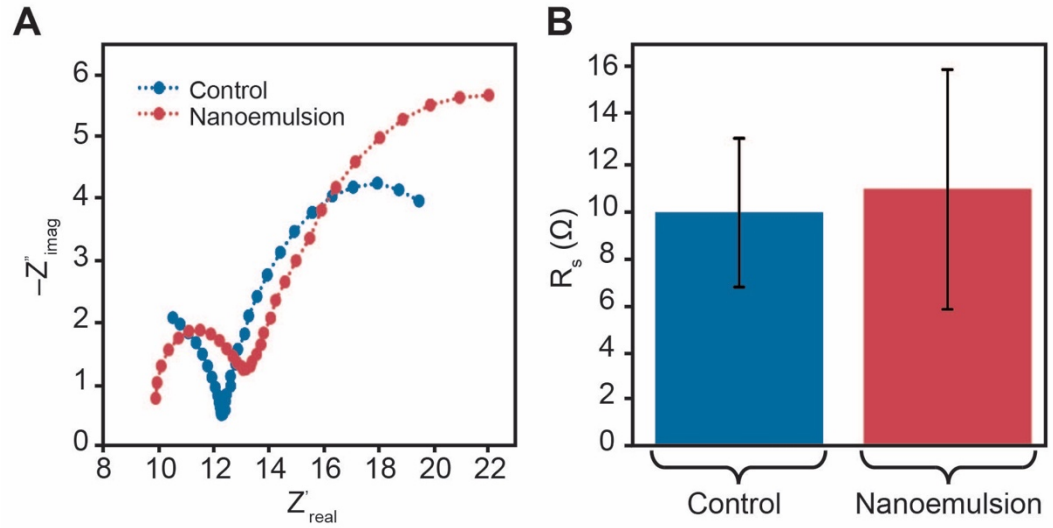


**Supplementary Fig. 5. a**, Representative Nyquist plots of Co-P alloy catalyst loaded on SS mesh substrate in solutions without (blue) and with (red) the introduction of PFC nanoemulsions. **b**, Statistical average of series resistance ($R_s$) in solutions without (blue) and with (red) the introduction of PFC nanoemulsions. $n \geq 16$, the errors denote SEM.

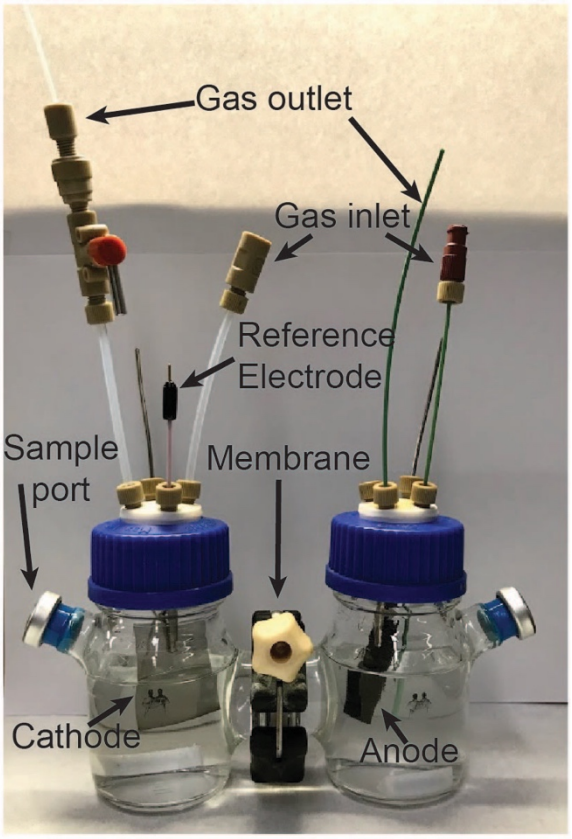


**Supplementary Fig. 6.** Experimental setup of bulk electrolysis depicting the electrodes, membrane separator, gas inlets/outlets, and sampling ports.

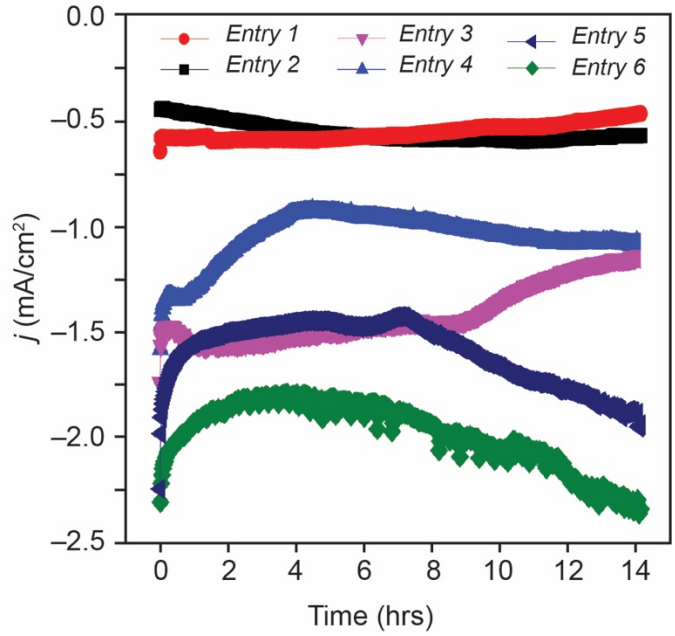


**Supplementary Fig. 7.** Representative chronoamperometry plots at varying current densities over the course of the first day during the bulk electrolysis experiments. The detailed experimental conditions of the denoted entries are shown in Supplementary Table 1.

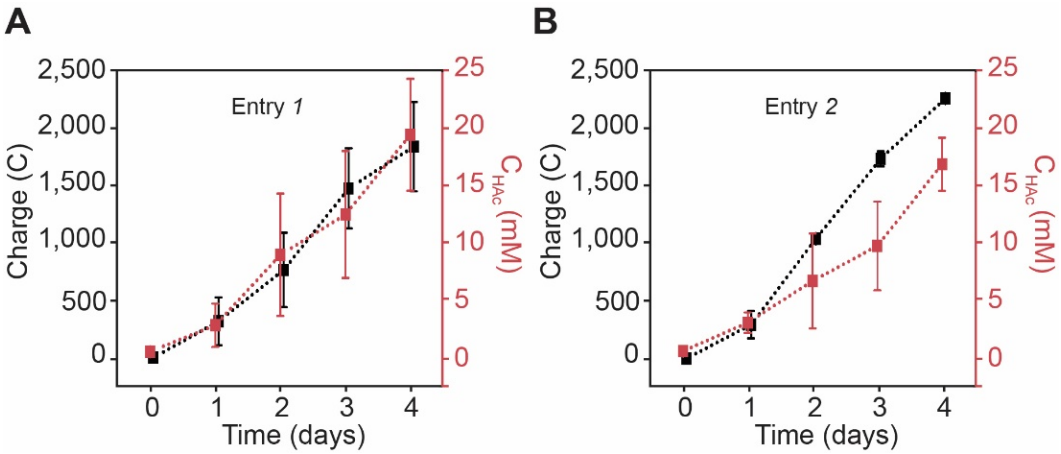


**Supplementary Fig 8.** Acetic acid (HAc) was selectively produced from $CO_2$ with electricity input without (**a**, entry *1* in Supplementary Table 1) and in the presence of nanoemulsion (**b**, entry *2* in Supplementary Table 1) at a current density of 0.54 mA/cm$^2$. The electric charge (black) and acetate concentrations (red) are plotted versus the duration of experiments. n = 3, the errors denote SEM.

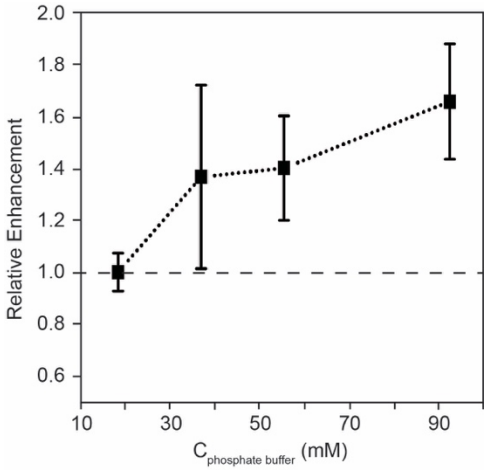


**Supplementary Fig 9.** Viability test of *S. ovata* in media of different concentrations of phosphate buffer. The relative enhancements of the accumulation of acetic acid by microbial $CO_2$ fixation are plotted against the concentrations of phosphate buffer. $n \geq 3$, the errors denote SEM.

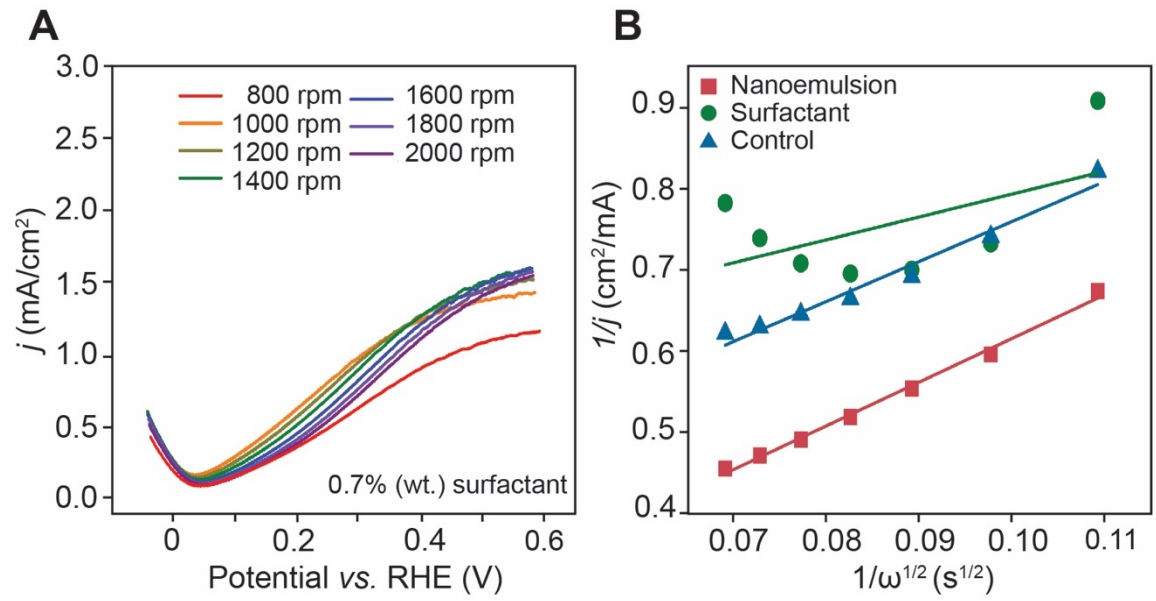


**Supplementary Fig 10. a**, Linear-sweep voltammograms of Pt RDE electrode under an environment of $H_2/CO_2$ (80/20) gas mixture (50 mV/s) with 0.7 wt% surfactant, which corresponds to 2.5% PFC nanoemulsion. The introduction of surfactants deactivates the hydrogen oxidation activity on Pt electrode. **b**, Koutechý-Levich plots of Pt RDE electrode at 0.1 V *vs.* RHE in the control medium (blue), with 0.5% PFC nanoemulsion (red), and with 0.14 wt% surfactant that was added when preparing 0.5% PFC nanoemulsion (green).

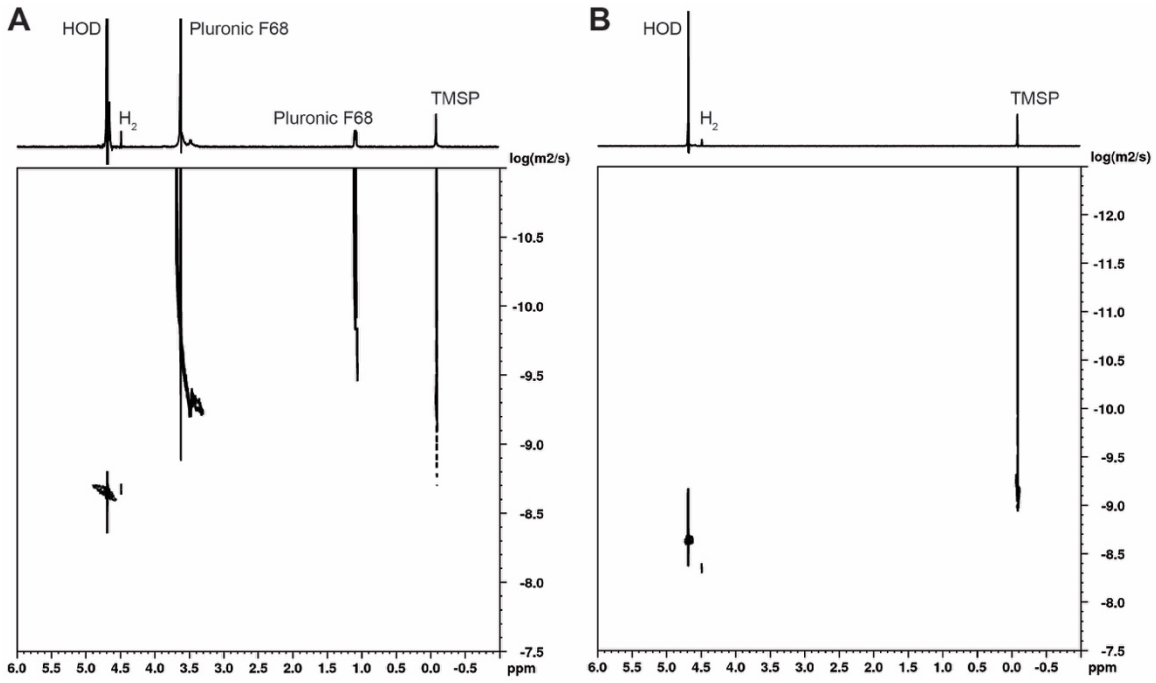


**Supplementary Fig 11.** DOSY $^{1}$H-NMR spectra with and without 0.5 % PFC nanoemulsion (**a** and **b**, respectively) in $D_2O$ under a $H_2$ pressure of 1 bar. TMSP-$d_4$ was added as an internal reference. The signals for $H_2$, TMSP-$d_4$, HOD impurities in $D_2O$ solvent, and the Pluronic F68 surfactant used for the PFC nanoemulsion are assigned.

**Supplementary references:**


1 Bard, A. J., Faulkner, L. R. *Electrochemical Methods: Fundamentals and Applications*. 2 edn, Ch. 9, page 331−344 (John Wiley & Sons, inc., 2001).

2 Han, P., Bartels, D. M., Temperature Dependence of Oxygen Diffusion in $H_2O$ and $D_2O$. *J. Phys. Chem.* **100**, 5597−5602 (1996).

3 Joback, K. G. & Reid, R. C. Estimation of Pure-Comonent Properties From Group-Contributors. *Chem Eng Commun* **57**, 233−243 (1987).

4 Liu, C. *et al.* Nanowire-Bacteria Hybrids for Unassisted Solar Carbon Dioxide Fixation to Value-Added Chemicals. *Nano Lett.* **15**, 3634−3639 (2015).

5 Nevin, K. P., Woodard, T. L., Franks, A. E., Summers, Z. M. & Lovley, D. R. Microbial Electrosynthesis: Feeding Microbes Electricity To Convert Carbon Dioxide and Water to Multicarbon Extracellular Organic Compounds. *mBio* **1**, e00103-10 (2010).

6 Sasaki, K. *et al.* Electrochemical biotechnologies minimizing the required electrode assemblies. *Curr. Opin. Biotechnol.* **50**, 182−188 (2018).

7 Nevin, K. P. *et al.* Electrosynthesis of organic compounds from carbon dioxide is catalyzed by a diversity of acetogenic microorganisms. *Appl. Environ. Microbiol.* **77**, 2882−2886, (2011).

8 Zhang, T. *et al.* Improved cathode materials for microbial electrosynthesis. *Energy Environ. Sci.* **6**, 217−224 (2013).

9 Nie, H. *et al.* Improved cathode for high efficient microbial-catalyzed reduction in microbial electrosynthesis cells. *Phys. Chem. Chem. Phys.* **15**, 14290−14294 (2013).

10 Aryal, N., Zhang, T., Tremblay, P.-L. *Microbial electrosynthesis for acetate production from carbon dioxide: innovative biocatalysts leading to enhanced performance*, Technical University of Denmark, (2017).

11 Aryal, N., Halder, A., Tremblay, P.-L., Chi, Q., Zhang, T. Enhanced microbial electrosynthesis with three-dimensional graphene functionalized cathodes fabricated via solvothermal synthesis. *Electrochim. Acta* **217**, 117−122 (2016).

12 Aryal, N., Tremblay, P.-L., Xu, M., Daugaard, A. E., Zhang, T. Highly Conductive Poly(3,4-ethylenedioxythiophene) Polystyrene Sulfonate Polymer Coated Cathode for the Microbial Electrosynthesis of Acetate From Carbon Dioxide. *Front. Energy Res.* **6**, 72 (2018).

13 Aryal, N., Tremblay, P. L., Lizak, D. M., Zhang, T. Performance of different Sporomusa species for the microbial electrosynthesis of acetate from carbon dioxide. *Bioresour. Technol.* **233**, 184−190 (2017).

14 Giddings, C. G., Nevin, K. P., Woodward, T., Lovley, D. R., Butler, C. S. Simplifying microbial electrosynthesis reactor design. *Front. Microbiol.* **6**, 468 (2015).

15 Bajracharya, S. *et al.* Carbon dioxide reduction by mixed and pure cultures in microbial electrosynthesis using an assembly of graphite felt and stainless steel as a cathode. *Bioresour. Technol.* **195**, 14−24 (2015).

16 Arends, J. B. A. *Optimizing the plant microbial fuel cell: diversifying applications and product outputs* Ph.D. thesis, Ghent University, Belgium, (2013).

17 Haas, T., Krause, R., Weber, R., Demler, M. & Schmid, G. Technical photosynthesis involving CO2 electrolysis and fermentation. *Nat. Catal.* **1**, 32-39 (2018).

18 Hu, P. *et al.* Integrated bioprocess for conversion of gaseous substrates to liquids. *Proc. Natl. Acad. Sci. U S A* **113**, 3773−3778 (2016).

19 Kantzow, C., Mayer, A. & Weuster-Botz, D. Continuous gas fermentation by Acetobacterium woodii in a submerged membrane reactor with full cell retention. *J. Biotechnol.* **212**, 11−18 (2015).